Volume 56
Number 84
28 October 2020
Pages 12673–12870

ChemComm

Chemical Communications

rsc.li/chemcomm

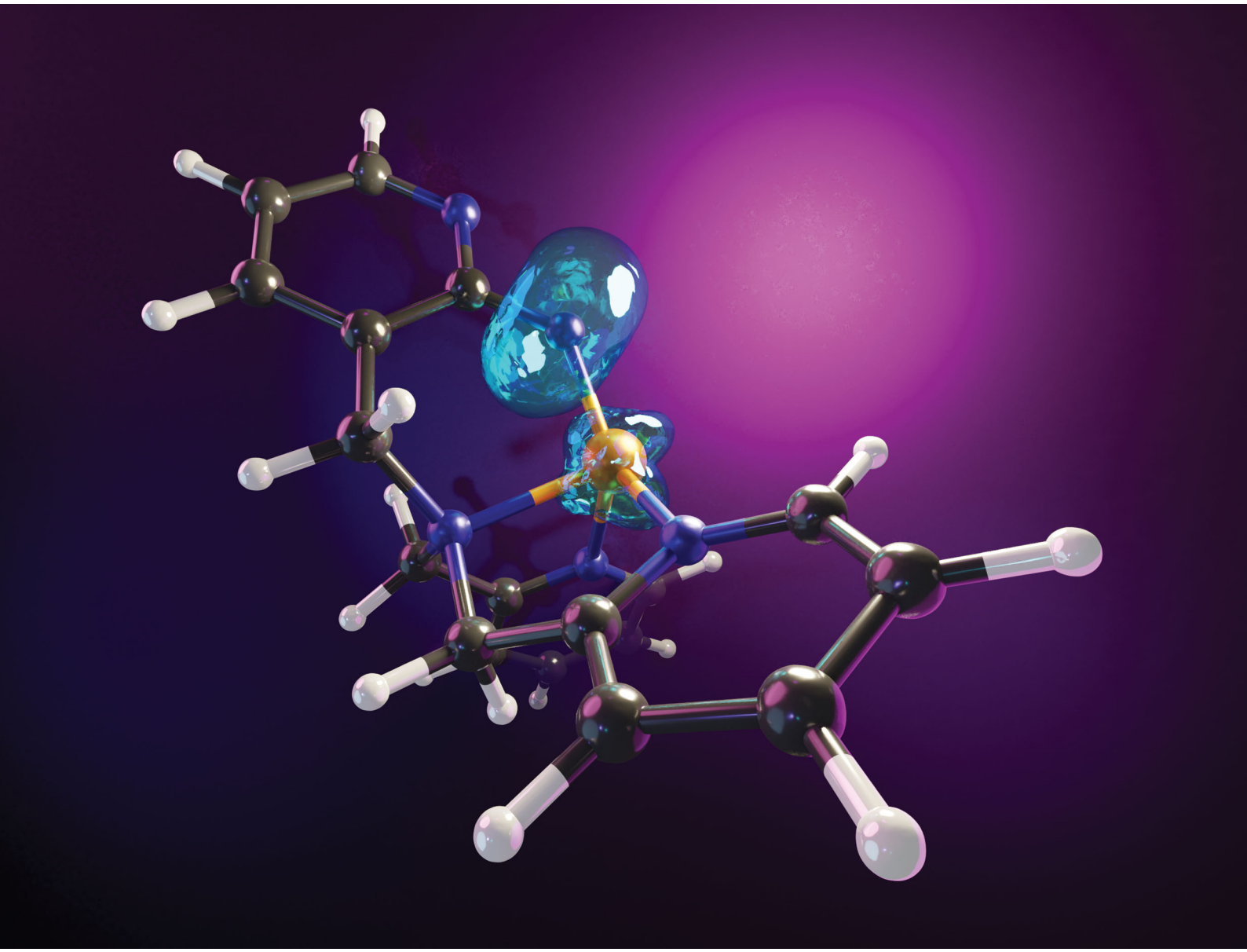

ISSN 1359-7345

ROYAL SOCIETY OF CHEMISTRY

COMMUNICATION

Noël R. M. de Kler and Jana Roithová

Copper arylnitrene intermediates: formation, structure and reactivity

ChemComm

COMMUNICATION

View Article Online
View Journal | View Issue

Cite this: *Chem. Commun.*, 2020, **56**, 12721

Received 30th July 2020,
Accepted 10th September 2020

DOI: 10.1039/d0cc05198e

rsc.li/chemcomm

Copper arylnitrene intermediates: formation, structure and reactivity†

Noël R. M. de Kler and Jana Roithová *

The mechanism of oxidation of arylamines by copper enzymes is not clarified yet. Here, we explored a reaction between a possible high-valent copper(II)-oxyl intermediate and arylamine. We have employed a TPA ligand (TPA = tris(2-pyridylmethyl)amine) with the NH_2 group in position 2 of one of the pyridine rings (TPA^{NH2}). This model system allows generation of $[(TPA^{NH2})Cu(O)]^+$ in the gas phase, which immediately undergoes a reaction between the arylamino group and the copper oxyl moiety. The reaction leads to elimination of H_2O and formation of a copper–nitrene complex. The structure of the resulting copper–nitrene complex was confirmed by infrared spectroscopy in the gas phase. We show that the copper–nitrene complex reacts by hydrogen atom transfer with 1,4-cyclohexadiene and by an order of magnitude faster by a double hydrogen atom transfer with ethanethiol and methanol. DFT calculations explain the formation of the copper nitrene as well as its reactivity in agreement with the experimental findings.

Aniline containing chemicals are a class of industrially produced chemicals that are toxic and harmful for the environment and need to be processed in an effective and economic approach. Oxidation of aniline substrates with enzymes is one of the green strategies to process aniline-based waste streams.[1,2] For example, multi-copper laccases are known for the oxidization of phenol- and aniline-type pollutants.[3] The large biodiversity of this enzyme family can be linked to different selectivities in the oxidations of various aniline and phenol derivatives.[4]

Laccases contain a mononuclear copper active site (T1) where the substrate oxidation takes place and a trinuclear copper cluster (T2/T3) that mediates four-electron reduction of oxygen to form water.[5–7] Both active sites are interconnected and thereby capable of oxidising various substrates. The electron transfer pathway has been well studied, but the overall oxidation mechanisms of aniline-type molecules is not clarified yet.[8–11] One of the possible scenarios is that the reaction with oxygen leads to the formation of reactive [copper(II)-oxyl]$^+$ (CuO^+) intermediates that subsequently oxidize aniline-type molecules. CuO^+ has been thought to be an important reactive species in enzymes such as particulate methane monooxygenases and polysaccharide monooxygenases.[12–14] However, copper(II)-oxyl complexes were not directly detected in solution because of their high reactivity; so far the only structural and reactivity assessment comes from gas phase studies.[15–19] The copper(II)-oxyl functionality is extremely reactive and oxidizes a broad spectrum of substrates even in the gas phase.[18] Here we will show how the nascent copper(II)-oxyl with the TPA ligand (TPA = tris(2-pyridylmethyl)amine) reacts with aniline-type molecules and investigate the mechanism of this oxidation.

The gaseous copper(II)-oxyl complexes can be best generated by electrospray ionization from their copper(II)chlorate precursors.[18] Electrospray ionization of methanol solution of $[(TPA)Cu(ClO_3)_2]$ yields initially the $[(TPA)Cu(ClO_3)]^+$ ion (**1a**, *m*/*z* 436) that can lose a ClO_2 radical in collision-induced dissociation (CID) to generate the desired $[(TPA)Cu(O)]^+$ complex (**2a**, Fig. 1a). The extreme reactivity of the copper(II)-oxyl species leads to oxidation of any C–H bond in proximity, which usually results in oxidation of the ligand.[15,16,20] Accordingly, we have spectroscopically proved that the nascent $[(TPA)Cu(O)]^+$ complex immediately activates a C–H bond of one of the pyridine ligands leading to an isobaric copper(I) complex with hydroxylated TPA ligand $[(TPA^{OH})Cu]^+$ (see Fig. S13, S14 and the related discussion in the ESI†).

In order to be able to study the arylamine oxidation, we had to link the amine functionality directly to the ligand. Hence, we functionalized the TPA ligand with one (TPA^{NH2}, **b**) and two ($TPA^{(NH2)2}$, **c**) amino group(s) according to a slightly modified literature procedure.[21–24] The precursor complexes $[Cu(TPA^{NH2})(ClO_3)]^+$ (**1b**, *m*/*z* 451) and $[Cu(TPA^{(NH2)2})(ClO_3)]^+$ (**1c**, *m*/*z* 466) were generated by electrospray ionization of a methanol solution of the corresponding ligand and $Cu(ClO_3)_2$ (Fig. S1, ESI†). Dissociation of complexes **1b** and **1c** (Fig. 1b and c)

Institute for Molecules and Materials, Radboud University, Heyendaalseweg 135, 6525 AJ Nijmegen, The Netherlands. E-mail: jana.roithova@ru.nl

† Electronic supplementary information (ESI) available: Supporting results obtained by NMR, MS and DFT calculations. See DOI: 10.1039/d0cc05198e

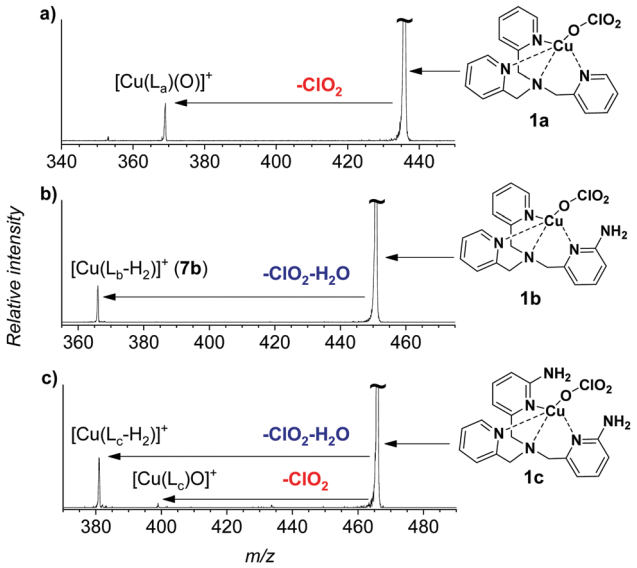

Fig. 1 Collision induced dissociation spectra of [(Ligand)Cu(ClO_3)]$^+$ complexes with xenon as the collision gas (P_{Xe} = 0.1 mTorr) at a collision energy of ~−4.2 eV in the centre of mass frame.

led to the expected ClO_2 radical elimination which, however, was associated with H_2O elimination. Presumably, the initial formation of [(TPA^{NH2})CuO]$^+$ (**2b**) or [(TPA$^{(NH2)2}$)CuO]$^+$ (**2c**) is followed by hydrogen atom transfer (HAT) from the amino group(s) leading to the formation of [Cu(TPA-nitrene)]$^+$ derivatives.

We have attempted to trap the [(TPA^{NH2})CuO]$^+$ (**2b**) reactive intermediate by slowing down the subsequent water elimination by deuteration of the amino group. However, we have observed selective elimination of ClO_2 and D_2O yielding again the nitrene product ions (Fig. S2, ESI†). For the complexes having the ligand with two amino groups, [Cu(TPA$^{(NH2)2}$)(ClO_3)]$^+$ (**1c**), we were able to trap a small amount of the ions prior to water elimination (**2c**, Fig. 1c), but the abundance was too small to perform further experiments with these ions. Most likely, both NH_2 groups participate in the HAT reactions leading to stabilization of the intermediate. In the following, we will focus on the system with ligand **b**.

We have further investigated the structure of the nitrene products. Exploratory DFT calculations suggest that H_2O elimination proceeds *via* a step-wise transfer of two hydrogen atoms from nitrogen to oxygen (Fig. 2). The reaction proceeds in the triplet state and it initially leads to copper(II)hydroxo complex ^{3}**3b** with an aminyl radical at the ligand. The second hydrogen atom transfer leads to copper(I) complex with the ligand bearing nitrene and coordinated to H_2O (^{3}**4b**). The alternative coupling of the OH and NH groups in ^{3}**3b** must be associated with a spin flip and leads to the hydroxyl aryl amine product ^{1}**8b** (see Fig. S15, ESI† for further details). Probably, due to the large internal energy, this complex cannot be isolated in the gas phase and instead the reaction proceeds further towards H_2O elimination. Either ^{1}**8b** or ^{3}**4b** can lose H_2O to form the detected nitrene ions.

We have further considered rearrangement of the initially formed nitrene ^{3}**5b** to more stable isomers.[25,26] ^{3}**5b** can undergo a ring expansion associated with a spin flip to form ^{1}**6b**, which is however 9.6 kcal mol^{-1} higher in energy than ^{3}**5b** (see also Fig. S15, ESI†). Alternatively, the nitrene ^{3}**5b** can change coordination mode and form isomer ^{3}**7b**, which is energetically preferred by 5.9 kcal mol^{-1}. For more possibilities see Fig. S15 and S16 in the ESI.†

In order to assign the structure of the formed nitrene product, we have measured the IR spectrum of the mass selected ion (*m*/*z* 366) using the helium tagging photodissociation technique (Fig. 3).[27,28] The spectra belong to the ions that are cooled to the ground vibrational state and are isolated under vacuum. Hence, they can be straightforwardly assigned based on comparison with theoretically predicted IR spectra of possible isomers (**5b**–**7b**). The experimental spectrum clearly agrees with the theoretical spectrum predicted for ^{3}**7b**. In particular, the bands at ~1505 cm^{-1} and ~1220 cm^{-1} correspond to the stretching vibrations of the pyridine ring bearing the nitrene functionality and to the stretching vibration of the nitrogen–pyridyl bond, respectively (highlighted in red and blue in Fig. 3). This vibration is not present in any other theoretical spectrum. The Cu–nitrene vibration is predicted at 600 cm^{-1}; this range is unfortunately not accessible in our instrument (more details in Fig. S3, ESI†). The isotopic shifts of this band are predicted by the theory as −3 cm^{-1} for ^{15}N labelling and −0.1 cm^{-1} for ^{65}Cu labelling, which makes the experimental confirmation of this bond next to impossible. This spectral range in photodissociation spectroscopy can be studied only with free electron lasers.[29]

The results show that the nascent copper(II)-oxyl intermediate readily reacts with aromatic amines to form copper-arylnitrenes. The reaction between an amine and copper(II)-oxyl is a new pathway of how to form copper nitrenes. The previous reports show the formation of copper nitrene complexes from copper azide precursors and from the reaction between a copper complex and PhI=NTs.[30–34] These reactive complexes are used for direct C–H amination reactions.[35,36] That is why we have also tested whether **7b** is reactive in hydrogen atom transfer reactions (Fig. S11, ESI†).

First, we tested the reactivity of **7b** toward 1,4-cyclohexadiene with a weak C–H bond. The reaction in the gas phase proceeds by single hydrogen atom transfer demonstrating that **7b** could indeed participate in direct C–H amination (Fig. 4). A KIE of ~2.5 was determined for HAT *via* the reaction of **7b** with partially deuterated 1,4-cyclohexadiene-1,2,3,4,5,6-d_6 in the gas phase (see Fig. S9, ESI† for more details). We also observe an adduct formation, which can result from the aziridination reaction, but we cannot confirm it based on the available data.

We reported previously that the reactive complexes preferring the proton-coupled electron transfer (PCET) mechanism for hydrogen atom transfer react more readily with thiols than with activated C–H bonds.[37] Hence, we tested this type of reactivity with ethanethiol (EtSH). The reaction of **7b** and EtSH leads to the formation of an adduct and to double hydrogen atom abstraction from EtSH (black spectrum in Fig. 4). The rate of the reaction is an order of magnitude larger than the rate of the reaction with 1,4-cyclohexadiene (see Fig. S11, ESI†).

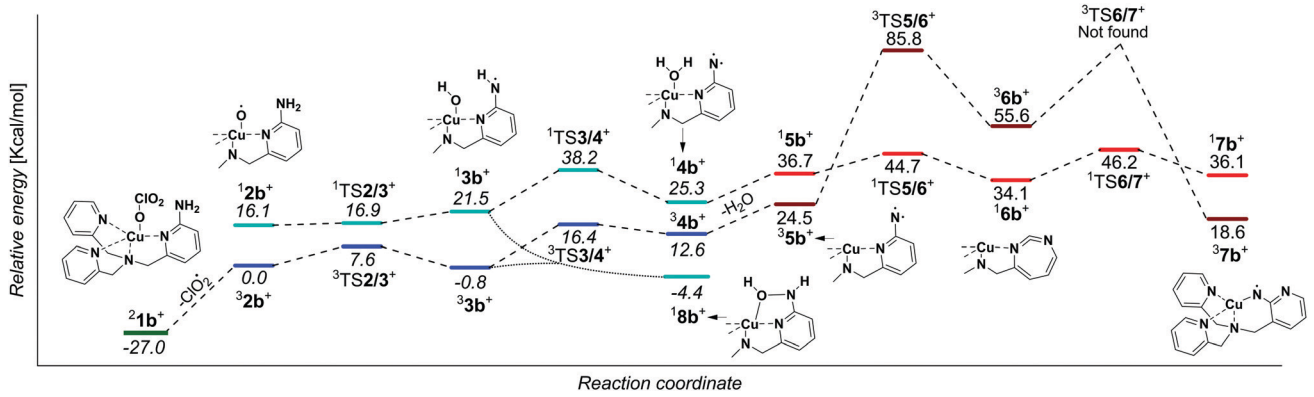

Fig. 2 Potential energy surface for the fragmentation and rearrangements of $[Cu(TPA^{NH2})(ClO_3)]^+$ (**1b**). The structures were calculated at the B3LYP/6-31+G* level and the relative energies refer to 0 K and are in kcal mol^{-1}. Some structures are displayed with a truncated ligand, but all calculations were performed with the full ligand.

The selective occurrence of double hydrogen atom transfer suggests that the aminyl radical formed from the nitrene in the first step can readily abstract a hydrogen atom from the carbon atom of the thiolate. The analogous dehydrogenation proceeds with methanol also (Fig. 4), which we investigated further in more detail.

The reaction of **7b** with methanol leads selectively to dehydrogenation of methanol without formation of an adduct (Fig. 4). The labelling experiments showed that the kinetic isotope effect (KIE) for the hydrogen atom abstraction from the oxygen atom is ~2.5, whereas KIE for the HAT from the methyl group is about 1 (compare the red, blue and green spectra in Fig. 4, detailed evaluation of KIEs using different approaches is in the ESI:† Fig. S5–S7). Exploratory DFT calculations confirm that the initial O–H bond activation is the rate determining step followed by HAT from the methyl group leading *via* a smaller energy barrier (Fig. 5 and Fig. S8, ESI†), while the first HAT proceeds in the triplet state, the second HAT from the methyl group is associated with a spin flip to the singlet state of the products.

The distribution of the spin density in **7b** shows that one of the unpaired electrons stays localized at the nitrene nitrogen atom. The electronic structure can be probably best represented as a mixture of two configurations: copper(I)/nitrene diradical and copper(II)/aminyl radical (note that an analogous structure has been found for copper(II)-oxyl complexes).[19] Hence, the first HAT with methanol leads to a complex between copper(II) methanolate and the aminyl radical. The final step leads to a copper(I) complex with an amine ligand.

In conclusion, we have shown that a copper(II)-oxyl complex reacts readily with arylamines by hydrogen atom transfer

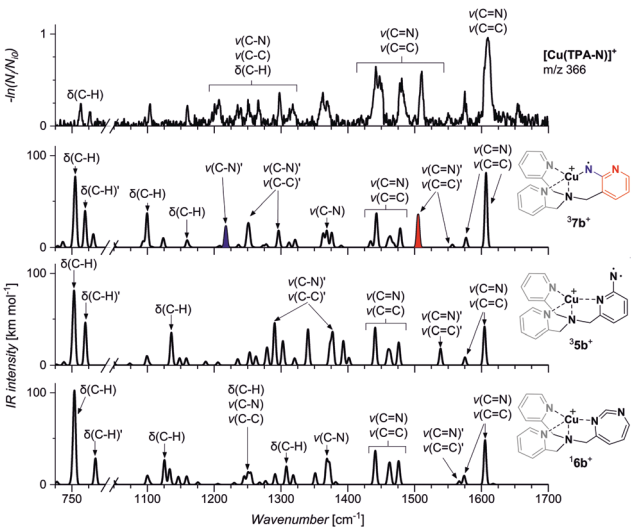

Fig. 3 Helium tagging infrared photodissociation spectrum of $[Cu(TPA-N)]^+$ (*m*/*z* 366) (top panel). Theoretical IR spectra of ^{3}**7b**, ^{3}**5b** and ^{1}**6b** were calculated for the optimized structures at the B3LYP/6-31+G* level and scaled by 0.97. δ(C–H), ν(C=C) and ν(C=N) correspond to the absorption bands in the pyridine rings whereas δ(C–H)′, ν(C=C)′ and ν(C=N)′ correspond to the absorption bands in the nitrene-pyridine ring.

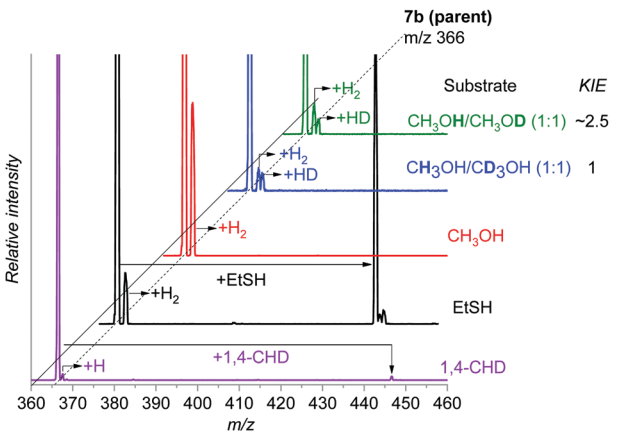

Fig. 4 Gas phase reactivity of **7b** with 1,4-cyclohexadiene (purple), ethanethiol (black), methanol (red), CH_3OH/CD_3OH (1 : 1) (blue), and CH_3OH/CH_3OD (1 : 1) (green). The experiments were performed at zero collision energy with a pressure of the reactant gas of 0.2 mTorr, except for 1,4-cyclohexadiene for which it was raised to 0.3 mTorr (see also Fig. S11, ESI†). The relative concentrations of the isotopically labelled methanols were determined by an association reaction with the $[Au(PMe_3)]^+$ cation (see the ESI† for details).

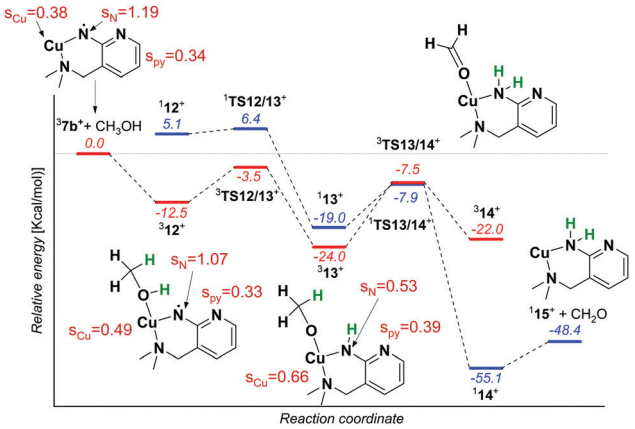

Fig. 5 Potential energy surface for the reaction of ^{3}**7b**$^+$ with methanol calculated at the B3LYP level with the 6-311+G(2d,p) basis set for copper and 6-31+G* basis set for all other atoms. The relative energies refer to 0 K and are in kcal mol^{-1}. The spin densities were obtained from Mulliken analysis at the B3LYP/6-311G(2d,p) level. The structures are displayed with a truncated ligand, but all the calculations were performed with the full ligand.

reactions. In the gas phase, this reaction leads to the formation of copper nitrene complexes. We have characterized the formed copper nitrene complex **7b** by its IR spectra and tested its reactivity. **7b** reacts with 1,4-cyclohexadiene by hydrogen atom transfer with a KIE of ~2.5. In addition, **7b** reacts readily with methanol or ethanethiol by two subsequent hydrogen atom transfers. With methanol, the hydrogen atom transfer from the oxygen atom is the rate determining step with the kinetic isotope effect of ~2.5.

The project was funded by the European Research Council (ERC CoG No. 682275).

Conflicts of interest

There are no conflicts to declare.

Notes and references

1 S. Witayakran and A. J. Ragauskas, *Adv. Synth. Catal.*, 2009, **351**, 1187–1209.
2 B. Yang, Y. Wang, Z. Liu, J. Liu and J. Cai, *J. Environ. Health Sci. Eng.*, 2019, **17**, 135–140.
3 F. Mirazizi, A. Bahrami, S. Soleimani Asl, A. Zaribafan, K. Haghbeen and S. Aminzadeh, *Int. J. Environ. Sci. Technol.*, 2018, **15**, 1679–1686.
4 R. Reiss, J. Ihssen, M. Richter, E. Eichhorn, B. Schilling and L. Thöny-Meyer, *PLoS One*, 2013, **8**, e65633.
5 E. I. Solomon, A. J. Augustine and J. Yoon, *Dalton Trans.*, 2008, 3921–3932.
6 E. I. Solomon, *Inorg. Chem.*, 2016, **55**, 6364–6375.
7 K. Ray, Y. M. Lee and W. Nam, *Coord. Chem. Rev.*, 2017, **334**, 25–42.
8 S. Shleev, A. Jarosz-Wilkolazka, A. Khalunina, O. Morozova, A. Yaropolov, T. Ruzgas and L. Gorton, *Bioelectrochemistry*, 2005, **67**, 115–124.
9 I. Pardo and S. Camarero, *Cell. Mol. Life Sci.*, 2015, **72**, 897–910.
10 S. M. Jones and E. I. Solomon, *Cell. Mol. Life Sci.*, 2015, **72**, 869–883.
11 A. Sekretaryova, S. M. Jones and E. I. Solomon, *J. Am. Chem. Soc.*, 2019, **141**, 11304–11314.
12 E. I. Solomon, D. E. Heppner, E. M. Johnston, J. W. Ginsbach, J. Cirera, M. Qayyum, M. T. Kieber-Emmons, C. H. Kjaergaard, R. G. Hadt and L. Tian, *Chem. Rev.*, 2014, **114**, 3659–3853.
13 V. V. Vu and S. T. Ngo, *Coord. Chem. Rev.*, 2018, **368**, 134–157.
14 M. O. Ross, F. MacMillan, J. Wang, A. Nisthal, T. J. Lawton, B. D. Olafson, S. L. Mayo, A. C. Rosenzweig and B. M. Hoffman, *Science*, 2019, **364**, 566–570.
15 D. Schröder, M. C. Holthausen and H. Schwarz, *J. Phys. Chem. B*, 2004, **108**, 14407–14416.
16 L. Jašóková, E. Hanikýřová, D. Schröder and J. Roithová, *J. Mass Spectrom.*, 2012, **47**, 460–465.
17 N. J. Rijs, P. González-Navarrete, M. Schlangen and H. Schwarz, *J. Am. Chem. Soc.*, 2016, **138**, 3125–3135.
18 G. Yassaghi, E. Andris and J. Roithov, *ChemPhysChem*, 2017, **18**, 2217–2224.
19 M. Srnec, R. Navrátil, E. Andris, J. Jašík and J. Roithová, *Angew. Chem., Int. Ed.*, 2018, **57**, 17053–17057.
20 N. Dietl, C. Van Der Linde, M. Schlangen, M. K. Beyer and H. Schwarz, *Angew. Chem., Int. Ed.*, 2011, **50**, 4966–4969.
21 M. Bhadra, J. Y. C. Lee, R. E. Cowley, S. Kim, M. A. Siegler, E. I. Solomon and K. D. Karlin, *J. Am. Chem. Soc.*, 2018, **140**, 9042–9045.
22 J. C. Mareque-Rivas, R. Prabaharan and R. T. Martín de Rosales, *Chem. Commun.*, 2004, 76–77.
23 D. E. Diaz, D. A. Quist, A. E. Herzog, A. W. Schaefer, I. Kipouros, M. Bhadra, E. I. Solomon and K. D. Karlin, *Angew. Chem., Int. Ed.*, 2019, **58**, 17572.
24 D. A. Quist, D. E. Diaz, J. J. Liu and K. D. Karlin, *J. Biol. Inorg. Chem.*, 2017, **22**, 253–288.
25 A. Maltsev, T. Bally, M. L. Tsao, M. S. Platz, A. Kuhn, M. Vosswinkel and C. Wentrup, *J. Am. Chem. Soc.*, 2004, **126**, 237–249.
26 C. Wentrup, *Acc. Chem. Res.*, 2011, **44**, 393–404.
27 J. Roithová and D. Gerlich, *Int. J. Mass Spectrom.*, 2013, **355**, 204–210.
28 J. Roithová, A. Gray, E. Andris, J. Jašík and D. Gerlich, *Acc. Chem. Res.*, 2016, **49**, 223–230.
29 L. Jašóková and J. Roithová, *Chem. – Eur. J.*, 2018, **24**, 3374–3390.
30 S. Kundu, E. Miceli, E. Farquhar, F. F. Pfaff, U. Kuhlmann, P. Hildebrandt, B. Braun, C. Greco and K. Ray, *J. Am. Chem. Soc.*, 2012, **134**, 14710–14713.
31 T. Corona, L. Ribas, M. Rovira, E. R. Farquhar, X. Ribas, K. Ray and A. Company, *Angew. Chem., Int. Ed.*, 2016, **55**, 14005–14008.
32 A. G. Bakhoda, Q. Jiang, J. A. Bertke, T. R. Cundari and T. H. Warren, *Angew. Chem., Int. Ed.*, 2017, **56**, 6426–6430.
33 J. Moegling, A. Hoffmann, F. Thomas, N. Orth, P. Liebhäuser, U. Herber, R. Rampmaier, J. Stanek, G. Fink, I. Ivanović-Burmazović and S. Herres-Pawlis, *Angew. Chem., Int. Ed.*, 2018, **57**, 9154–9159.
34 K. M. Carsch, I. M. DiMucci, D. A. Iovan, A. Li, S. L. Zheng, C. J. Titus, S. J. Lee, K. D. Irwin, D. Nordlund, K. M. Lancaster and T. A. Betley, *Science*, 2019, **365**, 1138–1143.
35 M. R. Fructos, S. Trofimenko, M. Mar Díaz-Requejo and P. J. Pérez, *J. Am. Chem. Soc.*, 2006, **128**, 11784–11791.
36 Y. M. Badiei, A. Dinescu, X. Dai, R. M. Palomino, F. W. Heinemann, T. R. Cundari and T. H. Warren, *Angew. Chem.*, 2008, **120**, 10109–10112.
37 E. Andris, R. Navrátil, J. Jašík, M. Puri, M. Costas, L. Que and J. Roithová, *J. Am. Chem. Soc.*, 2019, **140**, 14391–14400.

